RSC Advances

ROYAL SOCIETY OF CHEMISTRY

www.rsc.org/advances

RSC Advances

RSCPublishing

Paper

Criteria for the selection of support material to fabricate coated membranes for life support device

Cite this: DOI: 10.1039/xoxxoooooox

Yifan Yang, Dipak Rana*, Takeshi Matsuura, Songyuan Zheng and Christopher Q. Lan

Received ooth August 2014,
Accepted ooth xxxx 2014

DOI: 10.1039/xoxxoooooox

www.rsc.org/

Life support device, specifically vacuum desiccant cooling device requires hydrophobic micro-porous membranes with high liquid entry pressure of water (LEP_w), high mechanical strength and large vacuum distillation flux in the temperature range of 10-30 ºC. To achieve this goal, membranes were prepared by casting polyvinylidene fluoride (PVDF) on various non-woven fabric (NWF) materials using the immersion precipitation technique at the ambient temperature. Four porous polyester NWF materials were tested as the membrane support materials which were characterized by the SEM analysis and by measuring the contact angle and porosity. The PVDF coated membranes were also characterized by the SEM image analysis and LEP_w. Finally, the coated membranes were tested for vacuum membrane distillation (VMD) performance at a relatively low feed temperature of 30 ºC. Results of this study revealed a significant impact of NWF materials on VMD performance. A proper NWF material lead to a much enhanced VMD flux of the PVDF coated membrane that was approximately 15 times of the unsupported PVDF membrane. These results suggest that the spongy-like layer may have strong impacts on the flux of membrane distillation. The studies provide understanding VMD phenomenon and provide new insights for development of coated membranes used for the life support device.

1. Introduction

Membrane technology is of great interest in diverse applications such as sea water desalination, power generation and storage, greenhouse gases removal, semiconductor technology and medicine.[1] Membrane distillation is one of the most important applications for hydrophobic membranes, such as seawater desalination,[2,3] wastewater treatment,[4-6] extracting volatile organic compounds from dilute aqueous solutions,[7] degassing, etc. Hydrophobic polymeric membrane are also used in various setups like evaporative cooling[8,9] and vacuum desiccant cooling (VDC).[10] One of the popular options for producing this type of membrane is coating the hydrophobic polymeric layer over a porous support such as non-woven fabric (NWF) for strengthened mechanical property and resilience.[11] Permeation flux, mechanical strength, stability under operating condition and fouling resistance are some of the important properties affecting performance, as well as applicability and life-span of membranes.[12-15]

Many researchers have shown a great interest on optimization of the performance of the membrane with a coated layer recently and most of these works are focused on optimizing the coated layer. For instance, researchers have attempted to increase the flux by adding different non-solvent additives in the coagulation bath, adjusting the temperatures of the casting dope and coagulation bath,[16] adding surface modifying macromolecules into dope solution,[17] etc. However, it has been recognized that NWF not only improves mechanical strength, but other properties of NWF such as material, diameter and length of the fiber, pore size distribution, air transmission coefficient and surface roughness also play important roles in membrane performance.[18] Only a few studies have been addressed from the existing literature about the effects of backing material on the performance of the coated membrane. A notable exception is the work done by Lohokare et al.[19] on the effect of NWF on ultrafiltration membrane performance by comparing the woven and nonwoven supports. The effects of pretreatment of the backing material on the membrane performance were also studied by Zhang et al.[18] whereby two approaches to prepare a membrane of high rejection were proposed.

We recently reported that the hydrophobic membrane with high liquid entry pressure of water (LEP_w) (larger than 3 bar) is desirable for the application in personal cooling garment.[10] Izenson et al. [20] also reported the use of membranes of similar feature as part of their thermal and humidity control system for space suits. In their approach, they have used an expanded polytetrafluoroethylene (PTFE) laminate which can stand vacuum pressure while having sufficiently high vapor flux. Recognizing that PTFE is extremely inert as well as thermally stable, because of the nonpolar and nonreactive feature resulted from even distribution of fluorine atoms, it is however, on the other hand, difficult for anything to bond to it, and that's why PTFE (Teflon®) is well-known as a non-sticking and easy-to-clean product. This non-reactivity makes PTFE membrane less possible of fusing with other material, and therefore

less processaibility for setups which require membrane to be fabricated with other material. Polyvinylidene fluoride (PVDF), on the other hand, has similar feature with PTFE (hydrophobic, thermal stable, good chemical compatibility, etc.), and also have better adaptability for fabrication process.

For this reason, PVDF is an excellent membrane material choice for life support device. Design criteria is based on human trial tests of personal cooling garment application from our previous study, the desirable water vapour flux requirement is around 0.56 L/m^2h, and operating feed temperature is as low as around 30 °C, membrane is required to have high LEP (larger than 3 bar), improved water vapour flux, and improved robustness. Moreover, PVDF membrane, as a popular membrane material, has been widely studied in different applications for improved performance. Interested readers may find literatures on PVDF membranes.[21] Operating at low feed temperature (10-30 °C) for evaporative cooling purpose in life support device is relatively a new field of application, requiring for further deeper study for the new challenges. The presenting study is focused on these specific features requirement for PVDF development.

Recognizing the importance of support material that affects the performance of the coated membrane, and less studies have been reported from literature, the specific objective of this research is to investigate and understand the effect of backing materials on the morphology and vacuum membrane distillation (VMD) performance of coated PVDF membranes for life support device. However, more research is required for development of high performance membranes, which are a key component for VDC technology, improving high performance membranes with features including robustness and cost-effective purpose which will further enhance life support device development.

2. Experimental

Materials

Polyvinylidene fluoride (PVDF) (Kynar 740, Arkema Inc., Philadelphia, PA) was used as the base polymer. Dimethylacetamide (DMAc) supplied by Sigma-Aldrich of 99% purity was used as the solvent. Four non-woven fabric (NWF) polyester materials were used as the support materials for the membrane fabrication. Three of them, Hollytex® 3396, 3329, 3229 (Kavon Filter Products Co., Farmingdale, NJ), were kindly provided by the National Research Council, Ottawa, ON. The forth NWF support material was supplied by the Teijin Ltd. (Osaka, Japan), and quoted by its product number E055100-85. Those support materials are coded as 3396-support (A), E055100-85-support (B), 3329-support (C), and 3229-support (D) hereafter.

Polymer Characterization by Average Molecular Weights Measurement

The weight average molecular weight (Mw) and polydispersity index (PDI = Mw/Mn) of PVDF material was determined by the Younglin ACME 9000 gel permeation chromatography (GPC) in dimethyl formamide (DMF) at 40 °C with flow rate 0.5 ml/min on two polystyrene gel columns [PL gel 5 µm 10E 4 Å columns (300x7.5 mm)] connected in series to a Younglin ACME 9000 Gradient Pump and a Younglin ACME 9000 refractive index (RI) detector. The columns were calibrated against seven poly(methyl methacrylate) (PMMA) standard samples (Polymer Lab, PMMA Calibration Kit, M-M-10). The Mw and PDI of Kynar® 740 is 410 kD and 2.34, respectively.

Membrane Preparation

Flat sheet PVDF membrane was prepared by the immersion precipitation method [22] using the casting dope with a composition of PVDF 15 wt.% and water 1.25 wt.% in DMAc. To prepare the casting dope, PVDF, DMAc and water were mixed in a container, which was rotated at 180 rpm at 50 ºC for 24 h to ensure complete dissolution of the polymer. To make an unsupported membrane, the dope was cast at room temperature over a glass plate to a thickness of 0.25 mm, using a casting blade at a casting speed of around 6-7 cm/s, followed by immersing the cast film together with the glass plate into the coagulation bath (distilled water, ambient temperature) within 5 s. During gelation, the cast film solidified on the glass plate. The membrane was then taken out of the coagulation bath and dried at room temperature before being subjected to characterization and performance testing. This membrane is coded as PVDF-unsupported membrane.

When the membranes supported by the support materials were fabricated, a selected support material was used instead of the glass plate. The other fabrication procedure was the same as the unsupported membrane. The membranes so fabricated are coded as PVDF-3396-coated, PVDF- E055100-85-coated membrane, PVDF-3329-coated and PVDF-3229-coated, respectively.

Scanning Electron Microscopy (SEM) Measurement

The top surface of both non-woven polyester support materials and PVDF coated membranes was investigated by SEM (VegaII XMU, Tescan, PA). Au/Pd alloy was used to coat the samples by sputtering. SEM images were also used to obtain the pore size for PVDF coated membranes, followed by the ImageJ analysis proposed by Gribble et al.[23] and Zhao et al.[24] The ImageJ software (National Institute of Health, USA) was used in this study, assuming every pore is shaped like a circle.[25] Ten individual pores were chosen to calculate the pore size and the average value was recorded to minimize errors.

As well, the surface roughness of the support NWF material was investigated with the aid of the ImageJ software, following the approach discussed by Banerjee et al.[26] The micrographs were taken at 100× for backing materials and 15k× for the PVDF coated membranes; it has been proved by Banerjee et al. [26] that different magnifications of the micrographs provide similar results.

Porosity Measurement

The porosity of the support NWF materials was measured.[27] As the NWF polyester support materials are quite hydrophobic, water did not enter the pores, hence instead of water uptake, dimethylsulfoxide (DMSO) uptake tests were performed to calculate porosity. The support material was immersed in DMSO for 24 h to complete the wetting process. The weight of the support sample was measured before (dry) and after wetting with DMSO. The porosity can be calculated by the following equation:

$$\varepsilon(\%) = \frac{Total\ pore\ volume}{Total\ sample\ volume} = \frac{(m_s - m_d)}{A*L*\rho} \quad (1)$$

Where m_s and m_d are the weight of the wet and the dry sample, respectively.

The thickness of the support material was measured by a digital micro-meter before immersion into DMSO. Five

measurements were conducted for each type of support material to minimize the experimental error.

Contact Angle Measurement for Calculation of Surface Energy

The contact angle of the support materials and the PVDF coated membranes was measured by using A VCA Optima Surface Analysis System (AST Products Inc., Billerica, MA).The measurement was done by dropping 0.2 µL of liquid on the sample surface by using a micro-syringe (Hamilton Co., Reno, NV). Contact angles of ten randomly chosen locations were recorded and the average value was calculated to eliminate experimental errors.

Three liquids of different polar/nonpolar properties were used to measure the contact angel for the purpose of calculating the surface energy. The three liquids are deionized water, ethylene glycol (EG) and diiodomethane (DIM).

The surface free energy of the solid γ_S, was calculated, for each support material, by the Van Oss-Chaudhury-Good method proposed by Van Oss et al.[27] According to their method, γ_S is divided into two components, one includes the long-range interactions called the Lifshitz-van der Waals component (γ_S^{LW}), and the other contains the short-range interactions (acid-base) called the acid-base component (γ_S^{AB}). The equation is as followed:

$$\gamma_S = \gamma_S^{LW} + \gamma_S^{AB} = \gamma_S^{LW} + 2(\gamma_S^+\gamma_S^-)^{\frac{1}{2}} \qquad (2)$$

It is noted that γ_S^{AB} is further divided into γ_S^+ and γ_S^-, the Lewis acid and Lewis base component.

In order to calculate the surface free energy, the following Young-Dupré equation is used.[28]

$$(1+\cos\theta)\gamma_L = 2\sqrt{\gamma_S^{LW}\gamma_L^{LW}} + 2\sqrt{\gamma_S^+\gamma_L^-} + 2\sqrt{\gamma_S^-\gamma_L^+} \qquad (3)$$

Where θ is the contact angle, γ's have already been defined except for the subscript L which is for liquid.

The method to obtain the surface energy components γ_S^{LW}, γ_S^+ and γ_S^- of a given membrane is as follows. From the experimental contact angle data for three different liquids (water, EG and DIM) three simultaneous equations are written by using equation (3). In the equation numerical values are known for (γ_L, γ_L^{LW}, γ_L^- and γ_L^+) as summarized in Table 1. Then, the three simultaneous equations can be solved in terms of three unknowns: γ_S^{LW}, γ_S^+ and γ_S^-. As for the PVDF coated membranes, only the contact angle of water was measured.

Table 1. Van Oss, Chaudhury and Good Surface Tension Parameters of Liquids used in this Study

Liquid properties (mJ/m^2)	Water	Ethylene Glycol	Diiodomethane
γ_L	72.8	48	50.8
γ_L^{LW}	21.8	29	50.8
γ_L^+	25.5	1.92	0
γ_L^-	25.5	47	0

Liquid Entry Pressure of Water (LEP_w) Measurement

Membranes for the vacuum desiccant cooling device need to be operated under vacuum with concerns of potentially large local pressure, therefore the liquid entry pressure (LEP_w) of the VDC membrane is a governing parameter for it. The membrane with LEP_w lower than 3 bar is considered as a failure in this study. LEP_w was measured for all the PVDF coated and unsupported membranes using the LEP_w test set-up (Figure S1). The membrane cell was a stainless steel filter holder with a reservoir of 200 ml and an effective membrane area of 13.1 cm^2.

A dry membrane sample was placed on a sintered metal plate which was at the lower end of the membrane cell, and the liquid reservoir was filled with water. Compressed gas (nitrogen) was supplied to the reservoir from the nitrogen cylinder, and the pressure was increased by using a precision pressure regulator at a speed of 2 psi per 10 min until water started to flow continuously from the testing cell outlet. At this point, the LEP_w value was read from the pressure gauge. For each membrane sample, three measurements were made and the average value was recorded.

Permeation Flux Measurement by Vacuum Membrane Distillation (VMD) Setup

The equipment used for VMD consists of a cylindrical permeation cell with a feed chamber of about 300 mL wrapped with a heating tape for temperature control in a range of 22 to 35 ^oC (Figures S2). The temperature was measured by inserting a thermocouple to the feed chamber. The membrane was mounted to the bottom of the feed chamber. The vacuum was applied to the permeated side of the membrane via two cold traps. The permeate line was switched from cold trap 1 to cold trap 2 to collect the condensate after the system reached steady state in about 30 min. The feed side and the permeate side pressure were maintained at atmospheric pressure and 0.038 bar, respectively. The permate flux was calculated by:

$$J = \frac{W}{At} \qquad (4)$$

Where J, in unit of $\frac{kg}{m^2h}$ is the evaporation flux; W, in unit of kg, is the mass of vapor condensed in the trap 2; A, in unit of m^2, is the membrane area; t, in unit of h, is the operation time.

3. Results and discussion

The SEM top view and the two-dimensional pixel brightness graph of the four NWF materials are shown in Figure 1. From the figure it is observed that the fibers of the NWF material 3396 (coded as A in Figure 1) are flattened and most densely packed. The fiber diameter of 3396-support is the largest among all, and E055100-85-support (coded as B in Figure 1) appears to have the smallest fiber diameter while those of 3329-support (coded as C in Figure 1) and 3229-support (coded as D in Figure 1) are in between.

The intensities of pixels along a line drawn on the NWF material surface are shown at the right side of Figure 1, representing brightness intensity vs. distance. Looking at the figure, 3396-support (A) and E055100-85-support (B) are clearly distinguished from 3329-support (C) and 3229-support (D) by the following two features: (i) The average of the pixel brightness is higher for 3396-support (A) and E055100-85-support (B); The average pixel intensities of A, B, C, and D are 130, 130, 70, and 70, respectively; and (ii) The peaks of 3329-support (C) and 3229-support (D) are

broader and reach the bottom (Gray value = 0) more frequently than 3396-support (A) and E055100-85-support (B), meaning that the void spaces of 3329-support (C) and 3229-support (D) are larger and penetrate deeply to the bottom.

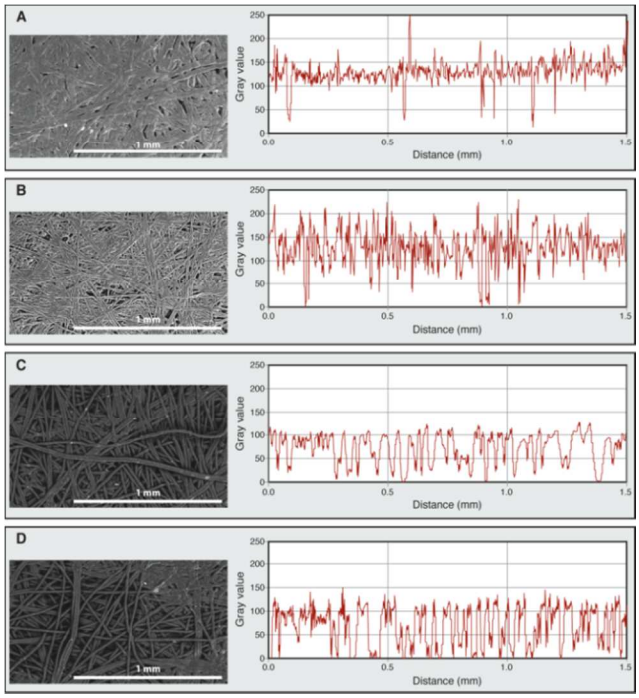

Fig. 1. Top SEM images for 3396-support (A), E055100-85-support (B), 3329-support (C), 3229-support (D), and the line profiles.

The contact angle data are plotted in Figure 2. It seems that 3396-support (A) and E055100-85-support (B) are remarkably different from the other two NWF materials with smaller contact angle for water and larger contact angle for diiodomethane (DIM). Since water is the most polar and DIM is the least polar liquid among the liquids used for the contact angle measurement, the above results indicate that the surface of 3396-support (A) and E055100-85-support (B) are less polar.

The calculated surface energies are summarized in Table 2. The NWF 3396-support (A) and E055100-85-support (B) have the two lowest values among all the NWF materials. Since the contact angle is largely affected by the surface morphology,[29] it is currently unknown if the surface energy represents the chemistry or the morphology of the NWF material. It can however be said the low surface energy enabled the wetting of the NWF material surface by DMAc, which is known to be a polar solvent.

The SEM images of the coated PVDF membrane top view are given in Figure 3. The surface of the PVDF-3329-coated membranes has developed some micro-cracks as can be observed clearly in Figure 3C. These SEM images can be used to evaluate the pore size using the ImageJ software.[23-25] The results presented in Table 3 show that the pore sizes of all the studied membranes were about 0.1 μm.

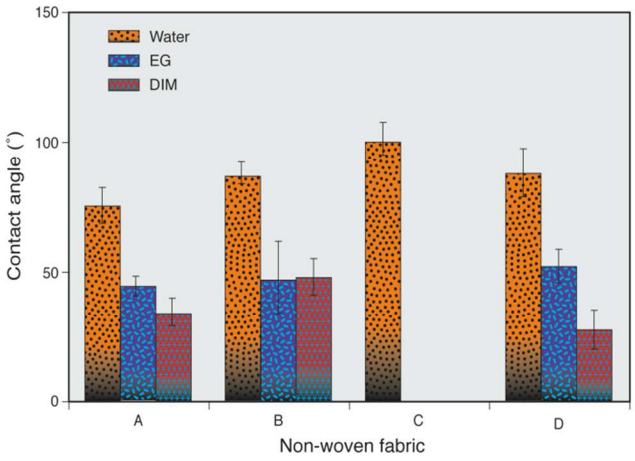

Fig. 2. Contact angles for water, ethylene glycol (EG), and diiodomethane (DIM) on four non-woven fabric materials. (Contact angles for EG and DIM on non-woven fabric material C are both zero.)

Table 2 Thickness, porosity, surface energy, and work of adhesion results for four support NWF materials.

NWF material	A	B	C	D
Thickness ($x10^{-4}$ m)	1.85	0.87	1.51	1.28
Porosity (%)	11.56 ±0.80	34.00 ±6.28	47.15 ±4.80	18.92 ±0.85
Surface energy (mJ/m^2)	44.23	37.46	53.53	48.15

The water contact angles are shown in Table 3 for all PVDF-coated membranes together with that of the unsupported PVDF membrane. The contact angles of PVDF-3396-coated (A-coated) and PVDF-E-055100-85-coated (B-coated) membrane and the unsupported membrane had similar contact angles, which were larger than that of the PVDF-3329-coated (C-coated) and PVDF-3229-coated (D-coated) membrane. These results suggest that the support materials did not have significant impact on the A-coated and B-coated membranes, however it affected the surface properties of the C-coated and D-coated membranes. This observation coincidences with the observation that some casting solution passed through the entire thickness of the support material in the fabrication of the C-coated and the D-coated membranes whereas in the case of the A-coated and B-coated membranes, casting solution did not pass through the entire thickness of the support material. It appears that the significant penetration of casting solution in fabrication of C-coated and D-coated membrane resulted in higher roughness of the membrane surface, which led to lower contact angles according to Wenzel's equation.[30] On the other hand, the limited penetration of casting solution in the fabrication of A-coated and B-coated membranes allowed the making of A-coated and B-coated

membranes with surface properties very similar to the supported membrane. This is consistent with the observation that extremely small LEP_w (less than 1 bar) was obtained with C-coated and D-coated membrane, which were confirmed by SEM images to have defects such as micro-cracks and pinholes. The significant penetration of casting solution through the C-support and D-support can be attributed to their surface unevenness, which is characterized by wide and deep valleys with thick fibers in the NWF. Thus the rough surface decreased the contact angle accordingly to Wenzel's equation, which predicts the contact angle on a rough surface would be smaller than on a smooth surface for the same material.[30] Nevertheless, it should be cautioned that the error ranges involved in the contact angles were large and the difference between the contact angles of composite membrane cast on different NWF materials may not be significant. It should be noted that although PVDF is a hydrophobic material, the contact angles of PVDF membranes were less than 90°. While this seems to contradict the intuitive thinking that the contact angle of a hydrophobic material should be equal or larger than 90°, however it is consistent with the observation of many other researchers.[31-34] For instance, the contact angle of UF membrane prepared from 19 wt% PVDF using DMAc solvent by phase inversion method was reported to be 83.64°. [33] Similarly, the contact angle was 78° for a UF membrane prepared from 16 wt% PVDF using DMF solvent by phase inversion method. [34]

Table 3 Contact angle, LEP_w, and VMD flux of the PVDF coated membranes.

Membrane	A-coated	B-coated	C-coated	D-coated	Unsupported
Pore size (μm)	0.092 ±0.015	0.11 ±0.019	0.14 ±0.013	0.09 ±0.019	N/A
Water contact angle (°C)	81.1 ±4.2	87.7 ±7.7	78.9 ±8.7	78 ±3.6	81.4 ±13.8
LEP_w (psi)	74 ±6	70 ±8	4.5 ±0.5	9.5 ±0.5	70 ±10
Flux at 30°C (L/m^2 h)	0.263 ±0.028	1.2325 ± 0.015	N/A	N/A	0.08 ±0.017

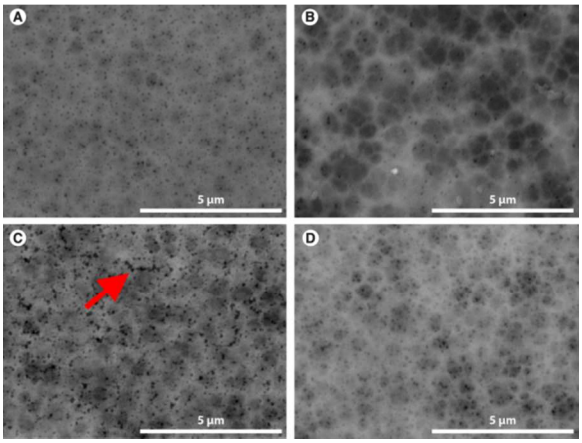

Fig. 3. Top SEM images for PVDF coated membranes and unsupported membrane. (A: PVDF-3396 coated; B: PVDF-E055100-85 coated C; PVDF-3329 coated; and D: PVDF-3229 coated membrane.)

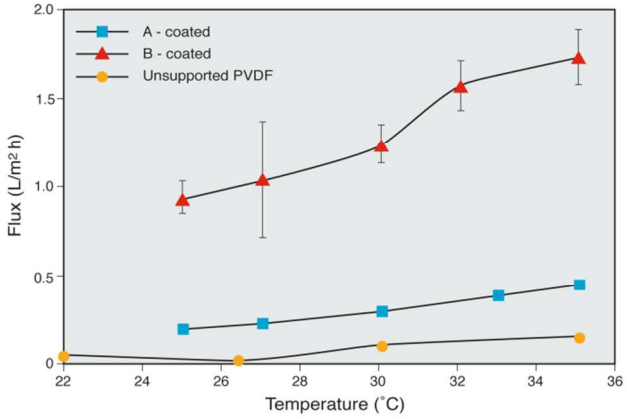

Fig. 4. Vapor flux of A-coated, B-coated, and unsupported PVDF membrane.

The VMD vapor fluxes are shown in Figure 4 for A-coated, B-coated and the unsupported membrane. The other two coated PVDF membranes (i.e., C-coated and D-coated) were unable to be used for VMD due to their low LEP_w values (less than 1 bar). The obtained vapor fluxes were 0.263 L/m^2h and 1.2325 L/m^2h for A-coated and B-coated membrane, respectively, at the feed temperature of 30 ºC. It is worth noting that the B-coated membrane exhibited a much higher flux (4.7 times higher at the feed temperature of 30 ºC) than A-coated membrane in the entire temperature range tested, i.e., from 25-35 ºC. This can be attributed to the smaller thickness and larger porosity of the B-support, as listed in Table 2, resulting in less resistance to the vapor transport than A-support.

It is worth noting that the unsupported membrane had a much lower VMD flux in the temperature range of 25-35 ºC (Figure 4) in comparison with both the A-coated and B-coated membranes. For instance, at 30 °C, the unsupported membrane had a flux of 0.08 L/m^2h, which was only one third of the flux of the A-coated membrane (0.263 L/m^2h), and 6.5% of the B-coated membrane (1.2325 L/m^2h). These results strongly indicate that properly selected NWF material could improve the structure of the coated membrane layer and therefore the overall VDM performance. One of such improvements could be that the pores of the supported membrane may not shrink as much as that of the unsupported membrane during the drying process in membrane fabrication due to the anchoring effects of the NWF material, minimizing pore size reduction.

B-coated membrane has significantly improved the fluxes comparing to the A-coated membrane. This could be explained by the NWF physical properties data shown in Table 2. B-support has less than half of the thickness comparing to that of A-support, which can enhance the flux by reducing the travelling distance for diffusing molecules. The B-support also has roughly three times the porosity than that of the A-support, and higher porosity means more pore channels open for diffusion, hence higher flux.[35]

Therefore, our studies expand the understanding of VMD phenomenon at the nano-scale and provide a guideline for the fabrication of coated membranes used for life support device. The prototypes of the life support VDC device will be tested with human subjects and the mathematical models will be developed to describe the mass and heat transfer in the VDC device. Improvement in the design of life support VDC device is expected to greatly increase the reliability, cooling capacity, work duration and cost-effectiveness and hence pave the way to its commercialization.

4. Conclusions

Membranes were fabricated by coating a thin-layer of PVDF via the immersion precipitation technique on four NWF materials to be used for VMD. The properties of the coated PVDF membranes depend largely on those of the NWF materials. A poor choice of NWF material selection may result in insufficient LEP_w due most likely to the formation of defective pores on the coated layer that may lead to the formation of micro-cracks. For the choice of proper NWF materials the following three requirements have to be satisfied: (i) The NWF material surface is smooth; (ii) The NWF material should be thin; (iii) The porosity of the NWL material is large, and (iv) The NWF material has relatively low surface energy.

The water vapor flux of the PVDF membrane coated on the E055100-85 (B) NWF material was 1.2325 L/m^2h, which was more than four times as high as that coated on 3396 (A) NWF, and was 15 times more than that of unsupported PVDF membrane. This study helps to develop a guideline for choosing a proper NWF support material for fabricating a hydrophobic PVDF membrane for life support VDC garment, which requires high LEP_w (over 3 bar) with high vapor flux, high mechanical strength and better processability. The flux of B-coated membrane is more than twice as much as the permeation flux (0.56 L/m^2h) desired for the life support device, which will significantly benefit the design of life support device by increasing the cooling performance. Processability is also improved significantly by the use of NWF for the backing material. At the same time, in contrast to the conventional thinking that the membrane skin-layer is the limiting factor governing the flux of VMD, these results suggest that the sponge-like layer of membrane, which is adjacent to the NWF, might also be a major contributing factor to mass transfer resistance in the supported membrane. Future studies in this regard are therefore warranted given the scarce information of the effects of sponge-layer structure on the performance of VMD.

Acknowledgements

Financial supports by the Natural Sciences and Engineering Research Council of Canada (NSERC) and the Canadian Institute of Health Research (CIHR). We would like to thank the Arkema Inc. (Philadelphia, PA) for the gift of polyvinylidene fluoride (Kynar®) polymer.

Notes and references

University of Ottawa, Department of Chemical and Biological Engineering, 161 Louis Pasteur Private, Ottawa, Ontario, K1N 6N5, Canada
Tel.: +1-613-562-5800 x 6085; fax: +1-613-562-5172.
E-mails: rana@uottawa.ca; rana@eng.uottawa.ca

† Electronic Supplementary Information (ESI) available: Experimental figures including liquid entry pressure of water measurement and permeation flux measurement by vacuum membrane distillation setup. See DOI: 10.1039/b000000x/

1. a) M. Tanaka and E. Sackmann, *Nature* 2005, **437**, 656; b) C. C. Striemer, T. R. Gaborski, J. L. McGrath and P. M. Fauchet, *Nature* 2007, **445**, 749; c) H. B. Park, B. D. Freeman, Z.-B. Zhang, M. Sankir and J. E. McGrath, *Angew. Chem. Int. Ed.* 2008, **47**, 6019; d) M. A. Shannon, P. W. Bohn, M. Elimelech, J. G. Georgiadis, B. J. Mariñas and A. M. Mayes, *Nature* 2008, **452**, 301; e) D. M. D'Alessandro, B. Smit and J. R. Long, *Angew. Chem. Int. Ed.* 2010, **49**, 6058; f) M. Elimelech and W. A. Phillip, *Science* 2011, **333**, 712; g) B. E. Logan and M. Elimelech, *Nature* 2012, **488**, 313; h) M. Carta, R. Malpass-Evans, M. Croad, Y. Rogan, J. C. Jansen, P. Bernardo, F. Bazzarelli and N. B. McKeown, *Science* 2013, **339**, 303; i) K. Celebi, J. Buchheim, R. M. Wyss, A. Droudian, P. Gasser, I. Shorubalko, J.-I. Kye, C. Lee and H. G. Park, *Science* 2014, **344**, 289.
2. G. C. Sarti, C. Gostoli and S. Matulli, *Desalination* 1985, **56**, 277.
3. M. Khayet, J. I. Mengual and T. Matsuura, *J. Membr. Sci.* 2005, **252**, 101.
4. S. Rosenberger, U. Krüger, R. Witzig, W. Manz, U. Szewzyk and M. Kraume, *Water Res.* 2002, **36**, 413.
5. P. Le-Clech, V. Chen and T. A. G. Fane, *J. Membr. Sci.* 2006, **284**, 17.
6. B. Van Der Bruggen, C. Vandecasteele, T. Van Gestel, W. Doyen and R. Leysen, *Environ. Prog.* 2003, **22**, 46.
7. S. Bandini, A. Saavedra and G. C. Sarti, *AIChE J.* 1997, **43**, 398.
8. H. T. El-Dessouky, H. M. Ettouney and W. Bouhamra, *Chem. Eng. Res. Des.* 2000, **78**, 999.
9. D. W. Johnson, C. Yavuzturk and J. Pruis, *J. Membr. Sci.* 2003, **227**, 159.
10. Y. Yang, J. Stapleton, B. T. Diagne, G. P. Kenny and C. Q. Lan, *Appl. Therm. Eng.* 2012, **47**, 18.
11. M. Khayet and T. Matsuura, *Membrane Distillation: Principles and Applications*, Elsevier, Amsterdam, 2011, Ch. 6.
12. A. Alpatova, E. Kim, X. Sun, G. Hwang, Y. Liu and M. Gamal El-Din, *J. Membr. Sci.* 2013, **444**, 449.
13. C. Feng, K. C. Khulbe, T. Matsuura, R. Gopal, S. Kaur, S. Ramakrishna, and M. Khayet, *J. Membr. Sci.* 2008, **311**, 1.
14. M. Nasir, H. Matsumoto, T. Danno, M. Minagawa, T. Irisawa, M. Shioya and A. Tanioka, *J. Polym. Sci. Polym. Phys. Ed.* 2006, **44**, 779.
15. M. Liu, J. Sun, Y. Sun, C. Bock and Q. Chen, *J. Micromech. Microeng.* 2009, **19**, 035028.
16. Y. Wang, B. Shi and X. Li, *Polym. Eng. Sci.* 2013, **53**, 1614.
17. a) H. Mahmud, J. Minnery, Y. Fang, V. A. Pham, R. M. Narbaitz, J. P. Santerre and T. Matsuura, *J. Appl. Polym. Sci.* 2001, **79**, 183; b) D. Rana and T. Matsuura, *Chem. Rev.* 2010, **110**, 2448; c) D. Rana, Y. Kim, T. Matsuura and H. A. Arafat, *J. Membr. Sci.* 2011, **367**, 110; d) Y. Kim, D. Rana, T. Matsuura and W.-J. Chung, *Chem. Commun.* 2012, **48**, 693; e) J. A. Prince, D. Rana, G. Singh, T. Matsuura, T. Jun Kai and T. S. Shanmugasundaram, *Chem. Eng. J.* 2014, **242**, 387; f) D. Rana, R. M. Narbaitz, A.-M. Garand-Sheridan, A. Westgate, T. Matsuura, S. Tabe and S. Y. Jasim, *J. Mater. Chem. A* 2014, **2**, 10059.
18. J. Zhang, Z. Wang and W. Li, *Desalin. Water Treat.* 2014, DOI: 10.1080/19443994.2013.831786.

19. H. R. Lohokare, Y. S. Bhole and U. K. Kharul, *J. Appl. Polym. Sci*. 2006, **99**, 3389.
20. M. Izenson, W. Chen and G. Bue, 43rd International Conference on Environmental Systems, Vail, CO, 14-18 July, 2013. http://ntrs.nasa.gov/archive/nasa/casi.ntrs.nasa.gov/20130011144_2013010796.pdf
21. a) K. Y. Wang, T.-S. Chung and M. Gryta, *Chem. Eng. Sci.* 2008, **63**, 2587; b) S. Bonyadi, T. S. Chung and R. Rajagopalan, *AIChE J.* 2009, **55**, 828; c) H. Fan and Y. Peng, *Chem. Eng. Sci.* 2012, **79**, 94; d) D. Hou, G. Dai, J. Wang, H. Fan, L. Zhang and Z. Luan, *Sep. Purif. Technol.* 2012, **101**, 1; e) H. Savoji, D. Rana, T. Matsuura, S. Tabe and C. Feng, *Sep. Purif. Technol.* 2013, **108**, 196; f) Z. Chen, D. Rana, T. Matsuura, Y. Yang and C. Q. Lan, *Sep. Purif. Technol.* 2014, **133**, 303; g) G. Kang and Y. Cao, *J. Membr. Sci.* 2014, **463**, 145; h) A. Figoli, S. Simone, A. Criscuoli, S. A. Al-Jlil, F. S. Al-Shabouna, H. S. Al-Romaih, E. Di Nicolò, O. A. Al-Harbi and E. Drioli, *Polymer* 2014, **55**, 1296.
22. T. Matsuura, *Synthetic Membranes and Membrane Separation Processes*, CRC Press, Boca Raton, FL, 1994.
23. C. M. Gribble, G. P. Matthews, G. M. Laudone, A. Turner, C. J. Ridgway, J. Schoelkopf and P. A. C. Gane, *Chem. Eng. Sci.* 2011, **66**, 3701.
24. S. Zhao, Z. Wang, J. Wang and S. Wang, *Ind. Eng. Chem. Res.* 2014, **53**, 11468.
25. Image J. Available from: http://rsb.info.nih.gov/ij/, accessed: July, 2014.
26. S. Banerjee, R. Yang, C. E. Courchene and T. E. Conners, *Ind. Eng. Chem. Res.* 2009, **48**, 4322.
27. M. Khayet and T. Matsuura, *Ind. Eng. Chem. Res.* 2001, **40**, 5710.
28. C. J. Van Oss, M. K. Chaudhury and R. J. Good, *Chem. Rev.* 1988, **88**, 927.
29. H. Y. Erbil, A. L. Demirel, Y. Avci and O. Mert, *Science* 2003, **299**, 1377.
30. R. N. Wenzel, *Ind. Eng. Chem.* 1936, **28**, 988.
31. L. Yan, Y. S. Li and C. B. Xiang, *Polymer* 2005, **46**, 7701.
32. X. Cao, J. Ma, X. Shi and Z. Ren, *Appl. Surf. Sci.* 2006, **253**, 2003.
33. F. Liu, N. A. Hashim, Y. Liu, M. R. M. Abed and K. Li, *J. Membr. Sci.* 2011, **375**, 1.
34. J. Ma, Y. Zhao, Z. Xu, C. Min, B. Zhou, Y. Li, B. Li and J. Niu, *Desalination* 2013, **320**, 1.
35. X. Shao, D. Dong, G. Parkinson and C.-Z. Li, *J. Mater. Chem. A* 2014, **2**, 410.